

# Salutary Effects of Estrogen Sulfate for Traumatic Brain Injury

Hyunki Kim,<sup>1</sup> Betul Cam-Etoz,<sup>2</sup> Guihua Zhai,<sup>1</sup> William J. Hubbard,<sup>2</sup>  
Kurt R. Zinn,<sup>1</sup> and Irshad H. Chaudry<sup>2</sup>

## Abstract

Estrogen plays an important role as a neuroprotector in the central nervous system (CNS), directly interacting with neurons and regulating physiological properties of non-neuronal cells. Here we evaluated estrogen sulfate ( $E_2$ -SO<sub>4</sub>) for traumatic brain injury (TBI) using a Sprague–Dawley rat model. TBI was induced via lateral fluid percussion (LFP) at 24 h after craniectomy.  $E_2$ -SO<sub>4</sub> (1 mg/kg BW in 1 mL/kg BW) or saline (served as control) was intravenously administered at 1 h after TBI ( $n = 5$ /group). Intracranial pressure (ICP), cerebral perfusion pressure (CPP), and partial brain oxygen pressure (pbtO<sub>2</sub>) were measured for 2 h (from 23 to 25 h after  $E_2$ -SO<sub>4</sub> injection). Brain edema and diffuse axonal injury (DAI) were assessed by diffusion tensor imaging (DTI), and cerebral glycolysis was measured by <sup>18</sup>F-labeled fluorodeoxyglucose (FDG) positron emission tomography (PET) imaging, at 1 and 7 days after  $E_2$ -SO<sub>4</sub> injection.  $E_2$ -SO<sub>4</sub> significantly decreased ICP, while increasing CPP and pbtO<sub>2</sub> ( $p < 0.05$ ) as compared with vehicle-treated TBI rats. The edema size in the brains of the  $E_2$ -SO<sub>4</sub> treated group was also significantly smaller than that of vehicle-treated group at 1 day after  $E_2$ -SO<sub>4</sub> injection ( $p = 0.04$ ), and cerebral glycolysis of injured region was also increased significantly during the same time period ( $p = 0.04$ ). However,  $E_2$ -SO<sub>4</sub> treatment did not affect DAI ( $p > 0.05$ ). These findings demonstrated the potential benefits of  $E_2$ -SO<sub>4</sub> in TBI.

**Key words:** DTI; estrogen; PET; TBI

## Introduction

TRAUMATIC BRAIN INJURY (TBI) accounts for >52,000 fatalities and 90,000 cases of premorbid loss of brain function in the United States annually.<sup>1,2</sup> TBI increases vasogenic fluid in the brain, resulting in cerebral edema that elevates intracranial pressure (ICP) and decreases cerebral perfusion pressure (CPP).<sup>3–5</sup> These lead to cerebral hypoxia and eventually ischemia.<sup>6</sup> Oxidative stress causes neuronal degeneration; therefore, partial brain oxygen pressure (pbtO<sub>2</sub>) has been used as a physiological biomarker to assess the severity of TBI.<sup>7</sup> Because nearly half of all TBI patients die within the first 2 h after injury, there is an urgent need for a novel therapeutic agent to induce instant salutary effects before patients arrive at the hospital.<sup>8,9</sup>

Estrogen sulfate ( $E_2$ -SO<sub>4</sub>) is the most abundant and potent endogenous estrogen in vertebrates, and it plays a pivotal role in neural network formation, neuronal activity, and synaptogenesis.<sup>10–13</sup>  $E_2$ -SO<sub>4</sub> reduces cortical contusion volumes, apoptosis, blood–brain barrier permeability, edema, levels of pro-inflammatory cytokines, and ICP.<sup>14</sup>  $E_2$ -SO<sub>4</sub> also increases CPP, improving neurological scores,<sup>15</sup> and protects neurons from oxidative stress.<sup>16</sup> Therefore,  $E_2$ -SO<sub>4</sub> has significant potential to serve as the first line treatment in TBI.

Diffusion tensor imaging (DTI) is a physiological magnetic resonance imaging (MRI) technique, which can measure the anisotropic diffusion of water molecules.<sup>17</sup> In white matter, water molecules diffuse along the nerve fibers, and the magnitude of the directional diffusion of water molecules can be quantitated with fractional anisotropy (FA) values. Therefore, the high FA values represent that the nerve fibers are aligned in the same direction. However, in the case of diffuse axonal injury (DAI), the fiber track is disrupted, and, therefore, the FA value is decreased. DTI can ascertain FA values, and has been used to assess DAI clinically.<sup>17–20</sup> DTI can also measure the isotropic diffusion of water molecules, which is quantitated as apparent diffusion coefficient (ADC) value.<sup>21</sup> The edema region contains many extracellular water molecules; therefore, it presents the higher ADC values than normal brain tissue. In a pilot clinical study, Zuccoli and coworkers recently reported that the mean ADC value of edematous regions was ~ 70% higher than that of normal-appearing brain tissue.<sup>22</sup>

<sup>18</sup>F-labeled fluorodeoxyglucose (FDG), a radiotracer used in positron emission tomography (PET) imaging, accumulates inside cells proportionally to glycolysis; therefore, it has been utilized for noninvasive assessment of cell viability in a target tissue.<sup>23</sup> <sup>18</sup>F-FDG uptake normalized to the body weight, referred to as standardized uptake value (SUV), has demonstrated reasonable

Departments of <sup>1</sup>Radiology and <sup>2</sup>Surgery, University of Alabama at Birmingham, Birmingham, Alabama.

reproducibility in an animal model.<sup>24</sup> <sup>18</sup>F-FDG PET imaging has been used in TBI patients,<sup>25</sup> and the lower uptake of <sup>18</sup>F-FDG was observed in severe TBI.<sup>26</sup>

The aim of this study was to determine the mechanism of the salutary effects of E<sub>2</sub>-SO<sub>4</sub> for TBI using a rat model, by measuring physiological parameters using clinical probes and quantitative parameters in DTI and <sup>18</sup>F-FDG PET imaging. We primarily focused on acute therapeutic intervention, to reduce cellular damage and brain edema within 24 h after E<sub>2</sub>-SO<sub>4</sub> administration.

## Methods

### Reagents

All reagents were from Fisher (Pittsburgh, PA) unless specified. E<sub>2</sub>-SO<sub>4</sub> was purchased from Sigma-Aldrich Co (St. Louis, MO). Lactated Ringer's solution was purchased from Baxter Healthcare Co (Deerfield, IL). <sup>18</sup>F-FDG was purchased from PETNET Solutions (Birmingham, AL). Carprofen was purchased from Pfizer Inc. (New York, NY), and prophylactic antibiotic enrofloxacin was purchased from Bayer Healthcare LLC (Shawnee Mission, KS). Ketamine was purchased from Vedco Inc. (St. Joseph, MO), and xylazine was purchased from LLOYD Inc. (Shenandoah, VA).

### Animal groups and modeling

All experimental procedures were in adherence to the National Institutes of Health (NIH) Guide for the Care and Use of Laboratory Animals, and approved by the Institutional Animal Care and Use Committee at the University of Alabama at Birmingham and ACURO. A total of seven groups of male Sprague–Dawley rats were employed ( $n=5$ /group;  $350\pm 25$  g;  $10\pm 2$  weeks old), and experimental TBI was induced with a fluid percussion device (VCU Biomedical Engineering, Richmond, VA), as previously described.<sup>15</sup> We have examined the effects of a single dose of E<sub>2</sub>-SO<sub>4</sub> at different concentrations (0.1–10 mg/kg BW, i.v., supraphysiological dose level) in a trauma-hemorrhage rat model, and the longest mean survival was observed at 1 mg/kg BW (data not shown). Therefore 1 mg/kg BW of E<sub>2</sub>-SO<sub>4</sub> (i.v., supraphysiological dose) was used in the present study. Table 1 summarizes the use of animals; four groups (groups 1–4) were used to measure physiological parameters including ICP, pbtO<sub>2</sub> and CPP, and three groups (groups 5–7) were used to measure imaging parameters. Groups 1–4 were: 1) sham group (no TBI) injected with vehicle (0.9% NaCl; i.v. 1 mL/kg BW), 2) sham group injected with E<sub>2</sub>-SO<sub>4</sub> (1 mg/kg BW in 0.9% NaCl; i.v. in a volume of 1 mL/kg BW), 3) TBI-induced group injected with vehicle, and 4) TBI-induced group injected with E<sub>2</sub>-SO<sub>4</sub>, respectively. Group 5 was a sham group

(three animals were injected with E<sub>2</sub>-SO<sub>4</sub>, and two animals were injected with vehicle), and groups 6 and 7 were TBI-induced groups treated with vehicle and E<sub>2</sub>-SO<sub>4</sub>, respectively. Sham animals were injected with either vehicle or E<sub>2</sub>-SO<sub>4</sub> at 25 h after craniectomy. TBI was induced at 24 h after craniectomy, and vehicle or E<sub>2</sub>-SO<sub>4</sub> was administered at 1 h after TBI. Physiological parameters (ICP, CPP, and pbtO<sub>2</sub>) were continuously measured for 2 h at 15 min intervals (from 23 to 25 h after E<sub>2</sub>-SO<sub>4</sub> or vehicle administration). *In vivo* imaging was applied at 1 and 7 days after administration.

### Craniectomy

Animals were anesthetized with 4% isoflurane, followed by an intraperitoneal injection of ketamine/xylazine mixture (100/10 mg/kg BW); then, anesthesia was maintained via ventilation with 1.5% isoflurane during surgery. Animals were placed on a heating pad to maintain normal body temperature throughout surgery. Animals were placed on a stereotaxic frame and the head was secured with ear bars. Burr hole and hub were prepared in the lateral skull at the junction of the sagittal, bregma, and lambda sutures. A 4.8 mm craniectomy was performed with a trephine over the right parietal cortex, midway between bregma and lambda, tangential to the sagittal suture. A rigid plastic injury tube (modified female Luer-lock 20G needle hub) was attached to the skull with cyanoacrylate adhesive over the open craniectomy with the intact dura, and a stabilizing screw was placed in a burr hole drilled rostral to bregma on the ipsilateral side. The injury tube and stabilizing screw were secured with dental acrylic. Then the scalp was sutured, and the animal was returned to a warmed recovery cage. All surgical procedures were performed using an aseptic technique.<sup>27</sup>

### TBI induction

The TBI-inducing device consisted of a Plexiglas cylinder (60 cm in length and 4.5 cm in diameter) filled with sterile water. A piston was mounted on O-rings at one end and an extracranial pressure transducer, EPN-0300A (Entran Devices Inc., Fairfield, NJ) connected to a storage oscilloscope, TDS 310 (Tektronix, Beaverton, OR), was attached to the opposite end. A 5 mm tube (internal diameter 2.6 mm) ending in a male Luer-lock was fitted at the end. TBI was induced by rapidly injecting a small volume of sterile saline into the closed cranial cavity over the right ipsilateral hemisphere with the fluid percussion device. Immediately thereafter, the animal was removed from the device, monitored for duration of apnea and unconsciousness, and re-sutured while receiving supplemental oxygen ventilation. The magnitude of the pressure pulse was measured by a pressure transducer, stored on an oscilloscope, and later converted to atmospheres. The pressure pulse was monitored and controlled in order to deliver an equivalent impact to each animal. Carprofen (5 mg/kg) and prophylactic antibiotic enrofloxacin (1 mg/kg) were intraperitoneally injected in each animal twice per day.

### Physiological parameter monitoring

Two femoral arteries were cannulated; the left artery to monitor mean arterial pressure (MAP) with a blood pressure analyzer (Digi-Med BPA blood pressure analyzer<sup>TM</sup>, MicroMed Inc., Louisville, KY), and the right artery to withdraw lactated Ringer's solution for fluid resuscitation. Animals were placed onto a stereotaxic frame including an incisor bar. The head was secured with ear bars, and body temperature was maintained via heat blanket (Animal Heating Pad, Davol Inc., Warwick, RI). After opening the scalp suture, ICP and pbtO<sub>2</sub> were measured by a Camino ICP monitoring probe (Integra NeuroScience, Plainsboro, NJ) and Licox oxygen catheter microprobe (Integra NeuroScience, Plainsboro, NJ), respectively. CPP was calculated by subtracting ICP values from MAP (CPP = MAP - ICP). Physiological parameters were monitored for 2 h, and animals were anesthetized with isoflurane (1 ~ 2%) during the entire procedure.

TABLE 1. TIME SCHEDULE OF TBI INDUCTION, DOSING, ICP/PBT<sub>2</sub>/CPP MEASUREMENT, AND IMAGING AFTER CRANIECTOMY IN EACH GROUP (N=5 PER GROUP)

	Time (h) after completing craniectomy				
	0h	24h	25h	47h-49h	167h-169h
Group 1 Craniectomy		Vehicle		ICP/pbtO <sub>2</sub> /CPP	
Group 2 Craniectomy		E <sub>2</sub> -SO <sub>4</sub>		ICP/pbtO <sub>2</sub> /CPP	
Group 3 Craniectomy	TBI	Vehicle		ICP/pbtO <sub>2</sub> /CPP	
Group 4 Craniectomy	TBI	E <sub>2</sub> -SO <sub>4</sub>		ICP/pbtO <sub>2</sub> /CPP	
Group 5 Craniectomy		Vehicle or E <sub>2</sub> -SO <sub>4</sub>		DTI/PET/CT	DTI/PET/CT
Group 6 Craniectomy	TBI	Vehicle		DTI/PET/CT	DTI/PET/CT
Group 7 Craniectomy	TBI	E <sub>2</sub> -SO <sub>4</sub>		DTI/PET/CT	DTI/PET/CT

TBI, traumatic brain injury; ICP, intracranial pressure; PbtO<sub>2</sub>, brain partial oxygen pressure; CPP, cerebral perfusion pressure; E<sub>2</sub>-SO<sub>4</sub>, estrogen sulfate; DTI, diffusion tensor imaging; PET, positron emission tomography.

## MRI

MR images were acquired with a 9.4T MR imaging system (Bruker BioSpin Corp., Billerica, MA) with a surface coil as receiver. The rat was placed in an animal bed equipped with circulating warm water to regulate body temperature, and was anesthetized using isoflurane (2–2.5%) during imaging. Anatomic imaging was acquired with a T2-weighted turbo spin-echo sequence (rapid acquisition with relaxation enhancement [RARE]). The detail parameters were as follows: repetition time (TR)=3000 ms; echo time (TE)=34 ms; RARE factor=4; field of view (FOV)=30×30 mm; matrix size=128×128; 30 slices with 1 mm thickness. DTI was performed using a modified Stejskal and Tanner spin-echo diffusion-weighted sequence with the following parameters: TR=3001 ms; TE=32 ms; matrix size=128×128; FOV=30×30 mm; six slices with 1 mm thickness. Image with  $b=0$  sec/mm<sup>2</sup> was acquired first, and then diffusion sensitizing gradients were applied along six directions as follows:  $[G_x, G_y, G_z]=[1, 1, 0], [1, 0, 1], [0, 1, 1], [-1, 1, 0], [0, -1, 1],$  and  $[1, 0, -1]$  with  $b=800$  sec/mm<sup>2</sup>. The diffusion tensor was represented by a 3×3 matrix with three eigenvalues  $\lambda_1, \lambda_2,$  and  $\lambda_3$ . The apparent diffusion coefficient (ADC) was calculated by

$$ADC = \frac{\lambda_1 + \lambda_2 + \lambda_3}{3},$$

and FA was calculated by

$$FA = \frac{\sqrt{3[(\lambda_1 - ADC)^2 + (\lambda_2 - ADC)^2 + (\lambda_3 - ADC)^2]}}{\sqrt{2(\lambda_1^2 + \lambda_2^2 + \lambda_3^2)}}.$$

On the ADC map, the edema region was determined as the area in the ipsilateral side having ADC values larger than the mean plus two standard deviations of ADC values on the contralateral side. The white matter was determined on FA maps as the region presenting higher FA values than the surrounding tissue. The relative FA value was calculated as the ratio of mean FA value in the region of white matter on the ipsilateral side to that on the contralateral side in each image slice, and the relative FA values of all six slices were averaged. ADC and FA values were calculated using computer software written with MATLAB (7.11.0, MathWorks, Inc.), and the region of interest (ROI) was segmented using conventional software, ImageJ, version 1.44p (National Institutes of Health, Bethesda, MD).

## PET/CT Imaging

PET/CT imaging was conducted using Triumph, a PET/CT dual-modality imaging system (GE, Northridge, CA) right after completing MR imaging. Radiographic CT imaging was performed together with PET imaging to identify the injured area. <sup>18</sup>F-FDG (65±1 MBq) in 300 μL phosphate buffered saline (PBS) was administered intravenously, and a 10 min scan was performed at 43±2 min after injection. Animals were under isoflurane anesthesia (2~2.5%) during dosing and imaging. The temperature of the animal bed in the Triumph scanner was maintained at 37°C during imaging. PET images were reconstructed with the maximum likelihood expectation maximization algorithm (10 iterations) in high-resolution mode. The axial FOV of PET images was set to 37.5 mm, and the axial spatial resolution and sensitivity at the center of FOV were 2.2 mm and 5.9%, respectively.<sup>28</sup> On CT imaging, the X-ray tube voltage and anode current were set to 75 kVp and 0.11 mA, respectively, and the axial FOV was 78.9 mm. A total of 256 projections were acquired in fly gantry motion mode for 1.07 min. The co-registration of PET and CT images was performed using ImageJ version 1.44p (National Institutes of Health, Bethesda, MD). In PET images, the SUV was calculated by  $SUV = (C \times W) / D$ , where  $C$  is tissue activity concentration (MBq/

mL),  $W$  is animal BW (g), and  $D$  is the administered dose (MBq). The relative SUV was determined by the ratio of mean SUV in the upper half of the brain to that of central region (~10 mm<sup>2</sup>) per each slice showing a skull opening, and the relative SUVs of four images (slice thickness: 1.175 mm) were averaged. The upper half of the brain region was manually determined based on the rat brain anatomy in CT images, whereas the central region was determined using shell analysis technique introduced in our previous study.<sup>29</sup>

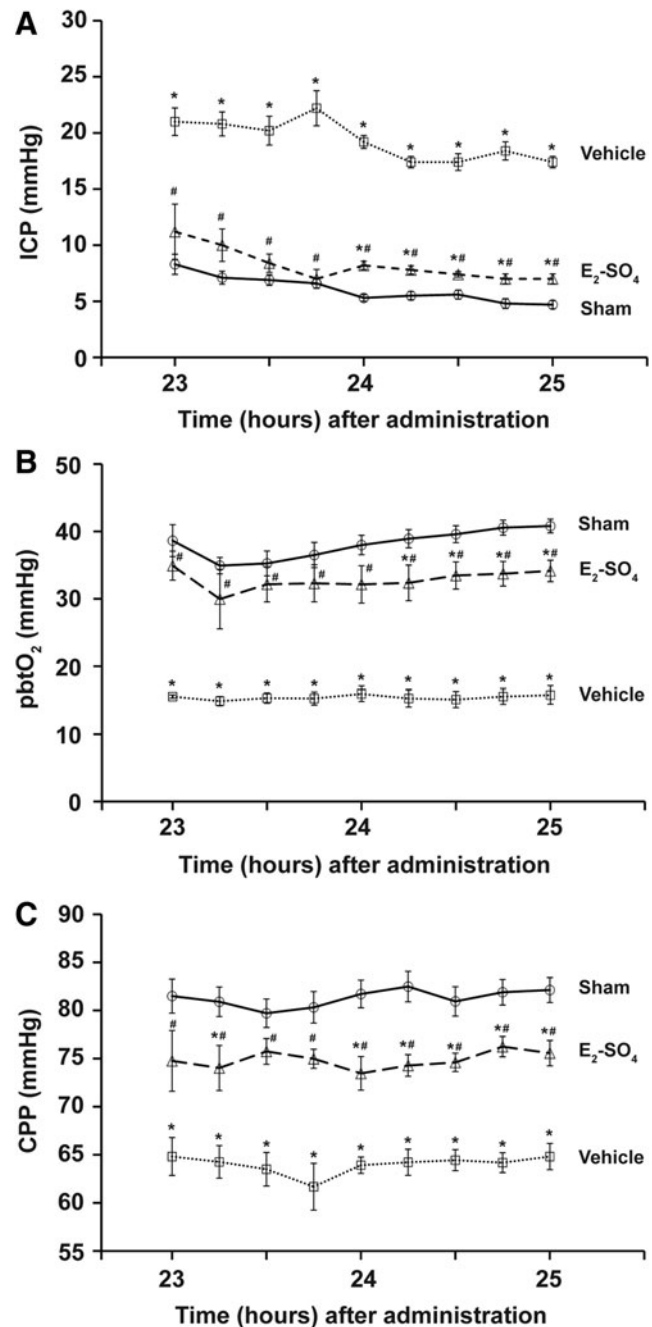


**FIG. 1.** Effect of estrogen sulfate (E<sub>2</sub>-SO<sub>4</sub>) treatment on physiological parameters following traumatic brain injury (TBI). (A) Intracranial pressure (ICP), (B) brain partial oxygen pressure (pbtO<sub>2</sub>), and (C) cerebral perfusion pressure (CPP) of sham, vehicle-, and E<sub>2</sub>-SO<sub>4</sub>-treated groups at nine different time points from 23 h to 25 h after administration. Asterisk and hashtag represent statistical difference from sham and vehicle-treated groups, respectively.



The segmentation of central brain region and SUV quantification were implemented using computer software written with Labview 2010 (National Instruments Co., Austin, TX). The upper half of the brain region was segmented using conventional software, ImageJ, version 1.44p (National Institutes of Health, Bethesda, MD).

### Statistical analysis

One-way ANOVA was implemented using SAS, version 9.4 (SAS Institute Inc., Cary, NC) to compare physiological parameters (ICP, CPP, and pbtO<sub>2</sub>) among sham, vehicle, and E<sub>2</sub>-SO<sub>4</sub> treated groups at each time point.<sup>30</sup> One way ANOVA was also used to compare edema size, relative FA value, and relative SUV among the groups. *P* values < 0.05 were considered significant, while applying Bonferroni correction for multiple comparisons.<sup>30</sup> Data are presented as means ± standard error.

## Results

### E<sub>2</sub>-SO<sub>4</sub> treatment decreased ICP and increased pbtO<sub>2</sub> and CPP

Figure 1 shows the changes of three physiological parameters (ICP, pbtO<sub>2</sub>, and CPP) of sham, vehicle, and E<sub>2</sub>-SO<sub>4</sub>-treated groups from 23 to 25 h after administration. Data of the sham group injected with E<sub>2</sub>-SO<sub>4</sub> were not statistically different from data of those injected with vehicle; therefore, the data from the two sham groups were combined (*n* = 10). During the entire 2 h, ICP of the E<sub>2</sub>-SO<sub>4</sub>-treated group was significantly lower than that of vehicle group, whereas pbtO<sub>2</sub> and CPP of the E<sub>2</sub>-SO<sub>4</sub>-treated group were significantly higher than those of vehicle group.

### E<sub>2</sub>-SO<sub>4</sub> treatment decreased edema in injured brain region

Figure 2A shows the brain ADC maps of representative animals in sham, vehicle, and E<sub>2</sub>-SO<sub>4</sub>-treated groups at 1 and 7 days after

administration. The edema area is indicated with a yellow arrow in each figure part. Edema was observed in both the vehicle- and the E<sub>2</sub>-SO<sub>4</sub>-treated groups, but not in the sham group, confirming that craniectomy did not directly damage the brain. Figure 2B presents the averaged edema size of the three groups on days 1 and 7. On day 1, the edema size of the E<sub>2</sub>-SO<sub>4</sub>-treated group was 10.3 ± 2.1 mm<sup>3</sup>, which was significantly lower than that of vehicle group (23.9 ± 5.1 mm<sup>3</sup>; *p* = 0.04). On day 7, the edema size of the E<sub>2</sub>-SO<sub>4</sub>-treated group was 1.2 ± 0.7 mm<sup>3</sup>, which was also significantly lower than that of the vehicle group (10.4 ± 2.6 mm<sup>3</sup>; *p* = 0.01), but not different from the sham group (*p* = 0.15).

### E<sub>2</sub>-SO<sub>4</sub> treatment was not able to recover axonal diffusion injury in 7 days

Figure 3A shows the FA maps (upper half of brain) of representative animals in the sham, vehicle, and E<sub>2</sub>-SO<sub>4</sub> treated groups on 1 and 7 days after administration. The white matter of the side that underwent craniectomy is indicated with a white arrow in each figure part. Figure 3B shows the relative FA values of the three groups on days 1 and 7. The relative FA values of the sham group were significantly higher than those of the vehicle- and E<sub>2</sub>-SO<sub>4</sub>-treated groups on both days 1 and 7 (*p* < 0.05), but no difference was detected between vehicle and E<sub>2</sub>-SO<sub>4</sub>-treated groups (*p* > 0.05) on either day.

### E<sub>2</sub>-SO<sub>4</sub> treatment increased glycolysis in the injured brain region

Figure 4A shows the <sup>18</sup>F-FDG PET/CT brain images of representative animals in the sham, vehicle-, and E<sub>2</sub>-SO<sub>4</sub>-treated groups 1 and 7 days after administration, respectively. The intensity of PET images was normalized to their central value (central region value is presented as 100%). The region that underwent craniectomy is indicated with a yellow arrow in each figure part.

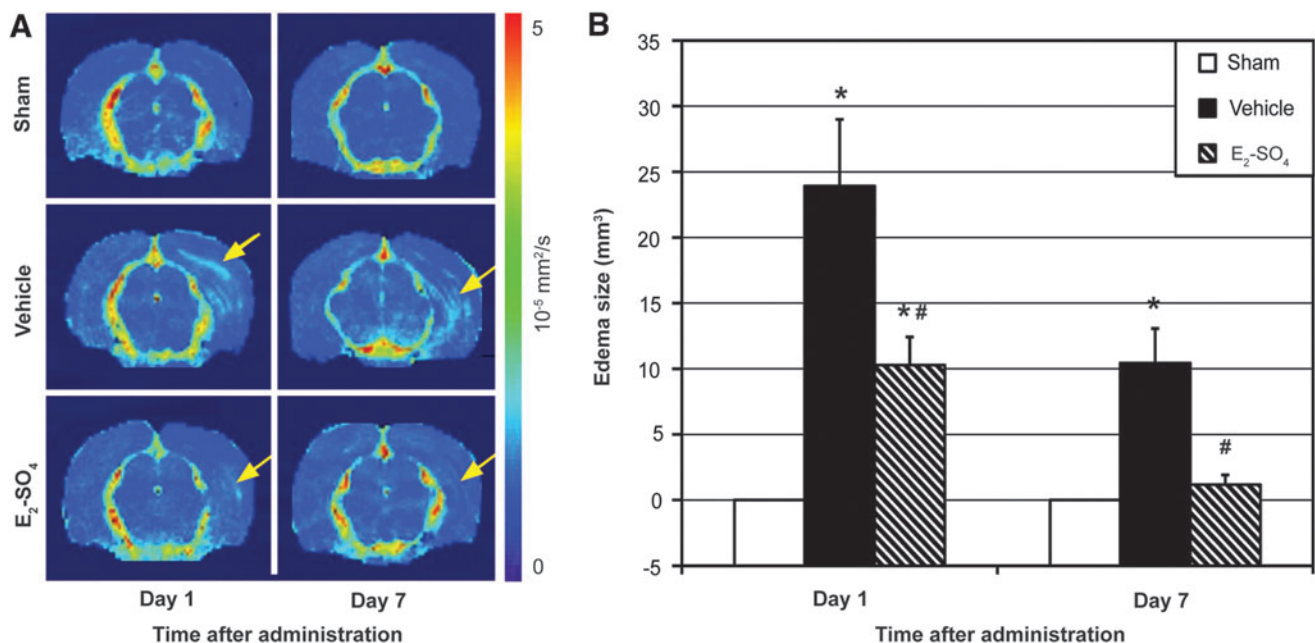


**FIG. 2.** Cerebral edema assessed by apparent diffusion coefficient (ADC) mapping. (A) Representative ADC maps (10<sup>-3</sup> mm<sup>2</sup>/sec) of sham, vehicle-treated, or estrogen sulfate (E<sub>2</sub>-SO<sub>4</sub>) treated animals at 1 or 7 days after administration. The edema is indicated with a yellow arrow in each figure part. (B) Mean edema size (mm<sup>3</sup>) of sham, vehicle-treated, or E<sub>2</sub>-SO<sub>4</sub>-treated group (*n* = 5 per group) at 1 or 7 days after administration. Asterisk and hashtag represent statistical difference from sham and vehicle-treated groups, respectively. Color image is available online at [www.liebertpub.com/neu](http://www.liebertpub.com/neu)

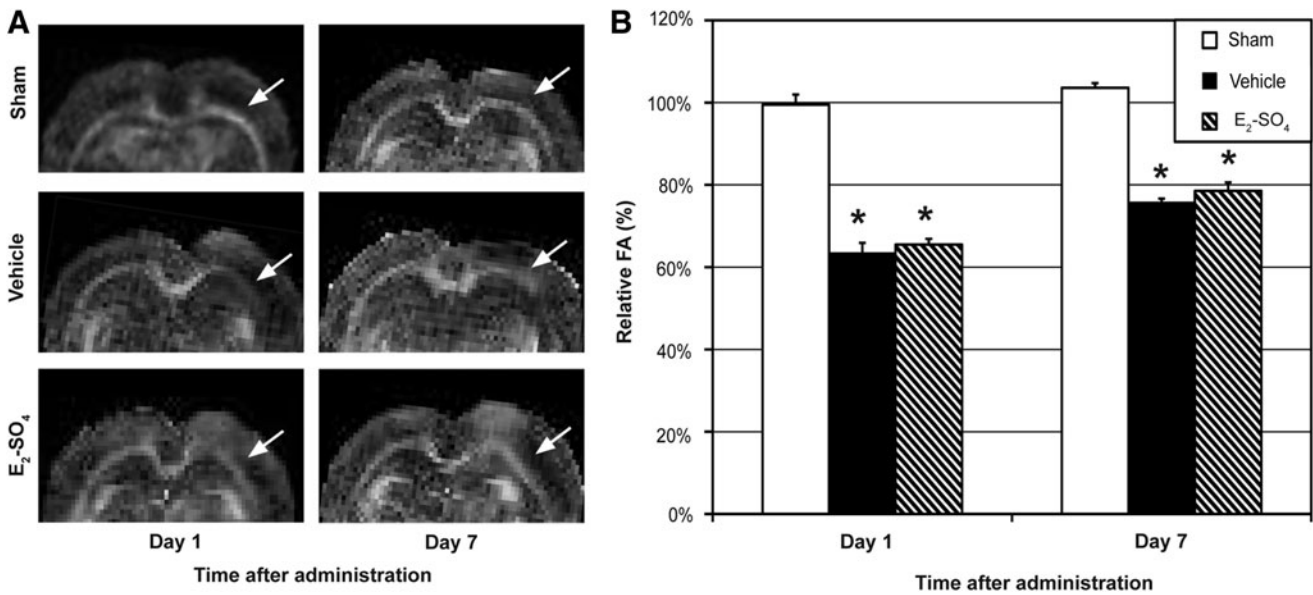


**FIG. 3.** Diffuse axonal injury assessed by fractional anisotropy (FA) mapping. **(A)** Representative FA maps of sham, vehicle-treated, or E<sub>2</sub>-SO<sub>4</sub>-treated animals at 1 day or 7 days after administration. The white matter in the side of craniectomy is indicated with a white arrow in each figure part. **(B)** Mean relative FA (ratio of FA signal in the white matter of the ipsilateral side to that of the contralateral side) of sham, vehicle-treated, or E<sub>2</sub>-SO<sub>4</sub>-treated group ( $n = 5$  per group) at 1 or 7 days after administration. Asterisk represents statistical difference from sham group.

Figure 4B presents the relative SUVs of the sham, vehicle-, and E<sub>2</sub>-SO<sub>4</sub>-treated groups on days 1 and 7, respectively. On day 1, the relative SUV of the E<sub>2</sub>-SO<sub>4</sub>-treated group was  $94.0 \pm 0.01\%$ , which was significantly higher than that of vehicle group ( $p = 0.04$ ), but not different from that of sham group ( $p = 0.12$ ). On day 7, however, no statistical difference was detected among the groups ( $p > 0.05$ ).

#### Discussion

To our knowledge, this is the first report for E<sub>2</sub>-SO<sub>4</sub> salutary effects in TBI, assessed by multimodal imaging and physiological parameters. A single dose of E<sub>2</sub>-SO<sub>4</sub> attenuated TBI severity within 24 h after administration, reducing pathological ICP and edema, while increasing pbtO<sub>2</sub>, CPP, and cerebral glycolytic metabolism.

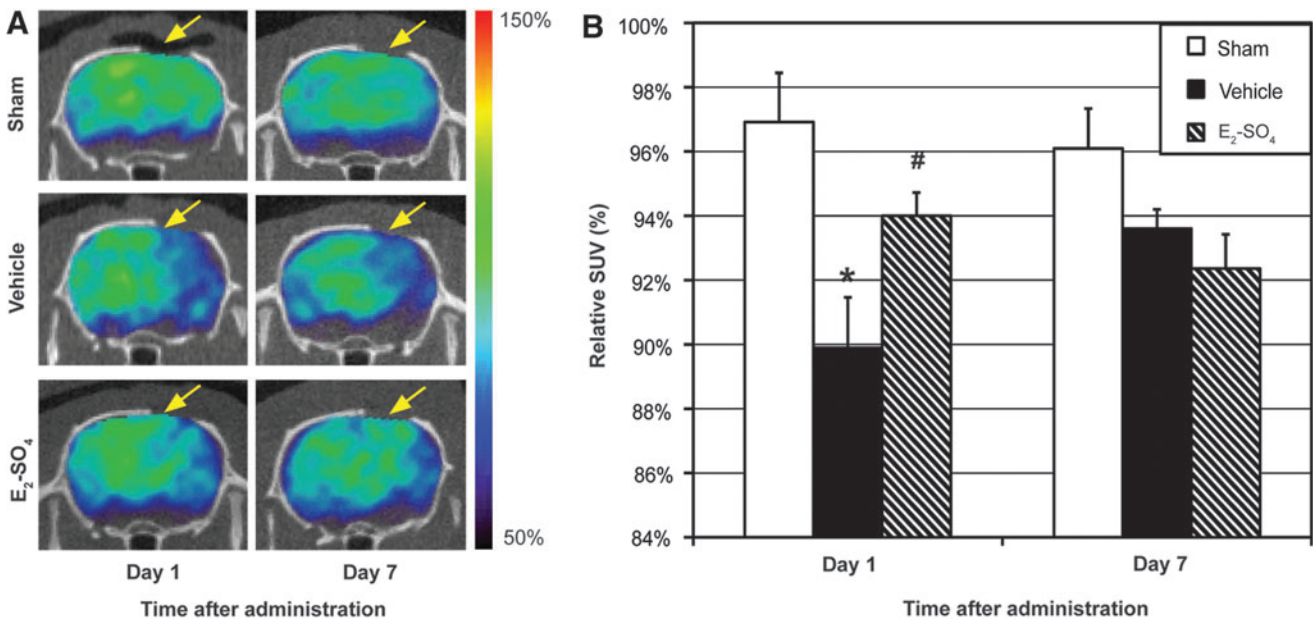


**FIG. 4.** Cerebral glycolysis assessed by <sup>18</sup>F-labeled fluorodeoxyglucose (<sup>18</sup>F-FDG) positron emission tomography (PET)/CT imaging. **(A)** Representative <sup>18</sup>F-FDG PET/CT images of sham, vehicle-treated, or E<sub>2</sub>-SO<sub>4</sub>-treated animals at 1 or 7 days after administration. The intensity of PET images is normalized to that of the central brain region. The area that underwent craniectomy is indicated with a yellow arrow in each figure part. **(B)** Mean relative standardized uptake value (SUV) (ratio of SUV of the upper half brain to that of central brain region) of sham, vehicle-treated, or E<sub>2</sub>-SO<sub>4</sub>-treated groups ( $n = 5$  per group) at 1 or 7 days after administration. Asterisk and hashtag represent statistical difference from sham and vehicle-treated groups, respectively. Color image is available online at [www.liebertpub.com/neu](http://www.liebertpub.com/neu)

$E_2$ -SO<sub>4</sub> increases vascular permeability and nitric oxide production, improving blood flow in the damaged brain area.<sup>11,12,14–16</sup> The increased microcirculation facilitates the transport of water molecules in the edematous region, verified by the reduction of ADC values, which results in the decrease of ICP. Consequently, CPP and pbtO<sub>2</sub> are enhanced, and, therefore, brain cell loss can be mitigated, as is shown by the increased relative SUV on the damaged area in FDG PET images.

Absolute SUV in FDG PET images of brain was, however, dominantly affected by animal mobility, and, therefore, could not be used to detect the improved brain cell activity by  $E_2$ -SO<sub>4</sub>. Recovery from TBI can lead to the increase of animal mobility, resulting in the increased uptake of <sup>18</sup>F-FDG in muscle tissue, and thereby its brain uptake can be somewhat decreased. In this study, markedly higher uptake of <sup>18</sup>F-FDG in masseter and pterygoid muscles was noticed in sham-treated animals, but not in TBI-induced ones. Therefore, it was necessary to calculate <sup>18</sup>F-FDG SUV in the brain relative to a reference region. The cerebellum has been commonly employed as the reference region to calculate the relative SUV in TBI rat models,<sup>31,32</sup> but poor signal to noise ratio (SNR) in the cerebellum region was often observed in this study; therefore, the central region of cerebrum was used instead. Therefore, in this study, the relative SUV measured the uniformity of <sup>18</sup>F-FDG distribution in the cerebrum, assuming that the central region was minimally affected by TBI.

$E_2$ -SO<sub>4</sub> was not able to alleviate DAI, measured by quantitative DTI, for 7 days after administration. Lee and coworkers showed that increased ICP was not associated with DAI among 36 TBI patients.<sup>33</sup> Also, Lafrenaye and coworkers confirmed that elevated ICP does not aggravate DAI using a TBI rat model.<sup>34</sup> Therefore, stabilizing ICP by  $E_2$ -SO<sub>4</sub> treatment may provide only limited impact on DAI. Meanwhile, it should be also noted that only a single dose of  $E_2$ -SO<sub>4</sub> was administered at 1 h after TBI in this study. Because the half-life of  $E_2$ -SO<sub>4</sub> is short, it is possible that administration of more than one dose of  $E_2$ -SO<sub>4</sub> or administration of estrogen with a longer half-life may provide a substantial effect on DAI. These possibilities, however, remain to be examined in future studies.

Early management of TBI is crucial to avoid pre-hospital hypoxia and hypotension. The intervention of primary brain injury with fast-acting drugs minimizes the secondary brain injury by maintaining adequate cerebral oxygenation and perfusion, which is significant for reducing morbidity and mortality.<sup>35</sup> However, traditional clinical treatments for TBI patients often require intravenous route of administration for a certain amount of time, which is not readily applicable in the location where the injury occurs, such as battlefields or natural disaster areas. Therefore, the prompt treatment with a single dose of a portable agent in an automated injector would be highly advantageous.

$E_2$ -SO<sub>4</sub> has both genomic and non-genomic protective effects following tissue injury, which include stabilizing the blood–brain barrier and neuron excitotoxicity, increasing cell-survival mediators, and modulating inflammatory process via decreasing pro-inflammatory and increasing anti-inflammatory molecules.<sup>36–39</sup> Treatment with estrogen following adverse additional circulatory conditions such as soft-tissue trauma and hemorrhage as well as organ ischemia and reperfusion has also been shown to have salutary effects.<sup>40–44</sup> Furthermore, it has been recently verified that early treatment with a single dose of  $E_2$ -SO<sub>4</sub> increased brain cell survival, while decreasing neuronal degeneration, apoptosis, and reactive astrogliosis in a TBI animal model.<sup>15</sup> Therefore, immediate treatment with a portable  $E_2$ -SO<sub>4</sub> administration kit for TBI

patients appears to be a promising approach to prevent permanent disability and irreversible neuronal damage.

## Conclusion

In conclusion, a single dose of  $E_2$ -SO<sub>4</sub> has successfully ameliorated TBI severity by reducing the pathological ICP and cerebral edema, and increasing pbtO<sub>2</sub>, CPP, and cerebral glycolysis in a rat TBI model. These data may support the future use of a portable administration kit of  $E_2$ -SO<sub>4</sub> for immediate TBI treatment in battlefields or civilian injury situations, to prevent permanent disability and irreversible neuronal damage, although more studies will need to be completed prior to clinical translation, such as comparing single versus repeated dosing, analyzing the response to a longer half-life agent, and assessing whether  $E_2$ -SO<sub>4</sub> has a clinically relevant therapeutic window.

## Acknowledgments

We give special thanks to Dr. Ahmar Ayub for TBI induction in rats, data collection, and analyses. Also, we thank Nicole Day and Tracy Niedzielko for their assistance in animal TBI induction, and Dr. Candace Floyd for letting us use her TBI induction instrument. This study was supported by the United States Army Medical Research and Materiel Command, Office of Congressional Directed Medical Research Program in TBI W81XWH-08-20153 of the Department of Defense to I.H.C.

## Author Disclosure Statement

No competing financial interests exist.

## References

1. Coronado, V.G., Xu, L., Basavaraju, S.V., McGuire, L.C., Wald, M.M., Faul, M.D., Guzman, B.R., and Hemphill, J.D. (2011). Surveillance for traumatic brain injury-related deaths—United States, 1997–2007. *MMWR Surveill. Summ.* 60, 1–32.
2. Langlois, J.A., Rutland-Brown, W., and Thomas, K.E. (2004). *Traumatic Brain Injury in the United States: Emergency Department Visits, Hospitalizations, and Deaths*. Centers for Disease Control and Prevention, National Center for Injury Prevention and Control: Atlanta.
3. Hiler, M., Czosnyka, M., Hutchinson, P., Balestreri, M., Smielewski, P., Matta, B., and Pickard, J.D. (2006). Predictive value of initial computerized tomography scan, intracranial pressure, and state of autoregulation in patients with traumatic brain injury. *J. Neurosurg.* 104, 731–737.
4. Stocchetti, N., Colombo, A., Ortolano, F., Videtta, W., Marchesi, R., Longhi, L., and Zanier, E.R. (2007). Time course of intracranial hypertension after traumatic brain injury. *J. Neurotrauma* 24, 1339–1346.
5. Unterberg, A.W., Stover, J., Kress, B., and Kiening, K.L. (2004). Edema and brain trauma. *Neuroscience* 129, 1021–1029.
6. DeWitt, D.S., Jenkins, L.W., and Prough, D.S. (1995). Enhanced vulnerability to secondary ischemic insults after experimental traumatic brain injury. *New Horiz.* 3, 376–383.
7. Murakami, Y., Wei, G., Yang, X., Lu, X.C., Leung, L.Y., Shear, D.A., and Tortella, F.C. (2012). Brain oxygen tension monitoring following penetrating ballistic-like brain injury in rats. *J. Neurosci. Methods* 203, 115–121.
8. Faul, M., Xu, L., Wald, M.M., and Coronado, V.G. (2010). *Traumatic Brain Injury in the United States: Emergency Department Visits, Hospitalizations and Deaths 2002–2006*. Centers for Disease Control and Prevention, National Center for Injury Prevention and Control: Atlanta.
9. Fearnside, M.R., Cook, R.J., McDougall, P., and McNeil, R.J. (1993). The Westmead Head Injury Project outcome in severe head injury. A comparative analysis of pre-hospital, clinical and CT variables. *Br. J. Neurosurg.* 7, 267–279.
10. Beyer, C. (1999). Estrogen and the developing mammalian brain. *Anat. Embryol. (Berl)* 199, 379–390.



11. Garcia-Segura, L.M., Chowen, J.A., Parducz, A., and Naftolin, F. (1994). Gonadal hormones as promoters of structural synaptic plasticity: cellular mechanisms. *Prog. Neurobiol.* 44, 279–307.
12. McEwen, B. (2002). Estrogen actions throughout the brain. *Recent Prog. Horm. Res.* 57, 357–384.
13. Roof, R.L., and Hall, E.D. (2000). Estrogen-related gender difference in survival rate and cortical blood flow after impact-acceleration head injury in rats. *J. Neurotrauma* 17, 1155–1169.
14. Liu, R., Liu, Q., He, S., Simpkins, J.W., and Yang, S.H. (2010). Combination therapy of 17beta-estradiol and recombinant tissue plasminogen activator for experimental ischemic stroke. *J. Pharmacol. Exp. Ther.* 332, 1006–1012.
15. Day, N.L., Floyd, C.L., D'Alessandro, T.L., Hubbard, W.J., and Chaudry, I.H. (2013). 17beta-estradiol confers protection after traumatic brain injury in the rat and involves activation of G protein-coupled estrogen receptor 1. *J. Neurotrauma* 30, 1531–1541.
16. Stein, D.G., and Hoffman, S.W. (2003). Estrogen and progesterone as neuroprotective agents in the treatment of acute brain injuries. *Pediatr. Rehabil.* 6, 13–22.
17. Watts, R., Thomas, A., Filippi, C.G., Nickerson, J.P., and Freeman, K. (2014). Potholes and molehills: bias in the diagnostic performance of diffusion-tensor imaging in concussion. *Radiology* 272, 217–223.
18. Bodanapally, U.K., Shanmuganathan, K., Saksobhavit, N., Sliker, C.W., Miller, L.A., Choi, A.Y., Mirvis, S.E., Zhuo, J., and Alexander, M. (2013). MR imaging and differentiation of cerebral fat embolism syndrome from diffuse axonal injury: application of diffusion tensor imaging. *Neuroradiology* 55, 771–778.
19. Ljungqvist, J., Nilsson, D., Ljungberg, M., Sorbo, A., Esbjornsson, E., Eriksson-Ritzen, C., and Skoglund, T. (2011). Longitudinal study of the diffusion tensor imaging properties of the corpus callosum in acute and chronic diffuse axonal injury. *Brain Inj.* 25, 370–378.
20. Seo, J.P., Kim, O.L., Kim, S.H., Chang, M.C., Kim, M.S., Son, S.M., and Jang, S.H. (2012). Neural injury of uncinate fasciculus in patients with diffuse axonal injury. *NeuroRehabilitation* 30, 323–328.
21. Seif, M., Lu, H., Boesch, C., Reyes, M., and Vermathen, P. (2014). Image registration for triggered and non-triggered DTI of the human kidney: Reduced variability of diffusion parameter estimation. *J. Magn. Reson. Imaging* [Epub ahead of print].
22. Zuccoli, G., Panigrahy, A., Sreedher, G., Bailey, A., Laney, E.J.T., La Colla, L., and Alper, G. (2014). Vasogenic edema characterizes pediatric acute disseminated encephalomyelitis. *Neuroradiology* 56, 679–684.
23. Farwell, M.D., Pryma, D.A., and Mankoff, D.A. (2014). PET/CT imaging in cancer: current applications and future directions. *Cancer* 120, 3433–3445.
24. Dandekar, M., Tseng, J.R., and Gambhir, S.S. (2007). Reproducibility of 18F-FDG microPET studies in mouse tumor xenografts. *J. Nucl. Med.* 48, 602–607.
25. Byrnes, K.R., Wilson, C.M., Brabazon, F., von Leden, R., Jurgens, J.S., Oakes, T.R., and Selwyn, R.G. (2014). FDG-PET imaging in mild traumatic brain injury: a critical review. *Front. Neuroenergetics* 5, 13.
26. Garcia-Panach, J., Lull, N., Lull, J.J., Ferri, J., Martinez, C., Sopena, P., Robles, M., Chirivella, J., and Noe, E. (2011). A voxel-based analysis of FDG-PET in traumatic brain injury: regional metabolism and relationship between the thalamus and cortical areas. *J. Neurotrauma* 28, 1707–1717.
27. Floyd, C.L., Golden, K.M., Black, R.T., Hamm, R.J., and Lyeth, B.G. (2002). Craniectomy position affects morris water maze performance and hippocampal cell loss after parasagittal fluid percussion. *J. Neurotrauma* 19, 303–316.
28. Prasad, R., Ratib, O., and Zaidi, H. (2010). Performance evaluation of the FLEX triumph X-PET scanner using the national electrical manufacturers association NU-4 standards. *J. Nucl. Med.* 51, 1608–1615.
29. Kim, H., Folks, K.D., Guo, L., Stockard, C.R., Fineberg, N.S., Grizzle, W.E., George, J.F., Buchsbaum, D.J., Morgan, D.E., and Zinn, K.R. (2011). DCE-MRI detects early vascular response in breast tumor xenografts following anti-DR5 therapy. *Mol. Imaging Biol.* 13, 94–103.
30. Neter, J., Kutner, M.H., Nachtsheim, J.C., and Wasserman, W. (1996). *Applied Linear Statistical Models*, 4th ed. The McGraw-Hill Companies, Inc.: Columbus.
31. Liu, Y.R., Cardamone, L., Hogan, R.E., Gregoire, M.C., Williams, J.P., Hicks, R.J., Binns, D., Koe, A., Jones, N.C., Myers, D.E., O'Brien, T.J., and Bouillere, V. (2010). Progressive metabolic and structural cerebral perturbations after traumatic brain injury: an in vivo imaging study in the rat. *J. Nucl. Med.* 51, 1788–1795.
32. Selwyn, R., Hockenbury, N., Jaiswal, S., Mathur, S., Armstrong, R.C., and Byrnes, K.R. (2013). Mild traumatic brain injury results in depressed cerebral glucose uptake: an (18)FDG PET study. *J. Neurotrauma* 30, 1943–1953.
33. Lee, T.T., Galarza, M., and Villanueva, P.A. (1998). Diffuse axonal injury (DAI) is not associated with elevated intracranial pressure (ICP). *Acta Neurochir. (Wien)* 140, 41–46.
34. Lafrenaye, A.D., McGinn, M.J., and Povlishock, J.T. (2012). Increased intracranial pressure after diffuse traumatic brain injury exacerbates neuronal somatic membrane poration but not axonal injury: evidence for primary intracranial pressure-induced neuronal perturbation. *J. Cereb. Blood Flow Metab.* 32, 1919–1932.
35. Chesnut, R.M., Marshall, L.F., Klauber, M.R., Blunt, B.A., Baldwin, N., Eisenberg, H.M., Jane, J.A., Marmarou, A., and Foulkes, M.A. (1993). The role of secondary brain injury in determining outcome from severe head injury. *J. Trauma* 34, 216–222.
36. Khaksari, M., Keshavarzi, Z., Gholamhoseinian, A., and Bibak, B. (2013). The effect of female sexual hormones on the intestinal and serum cytokine response after traumatic brain injury: different roles for estrogen receptor subtypes. *Can. J. Physiol. Pharmacol.* 91, 700–707.
37. Shahrokhi, N., Haddad, M.K., Joukar, S., Shabani, M., Keshavarzi, Z., and Shahozehi, B. (2012). Neuroprotective antioxidant effect of sex steroid hormones in traumatic brain injury. *Pak. J. Pharm. Sci.* 25, 219–225.
38. Siriphorn, A., Dunham, K.A., Chompoopong, S., and Floyd, C.L. (2012). Postinjury administration of 17beta-estradiol induces protection in the gray and white matter with associated functional recovery after cervical spinal cord injury in male rats. *J. Comp. Neurol.* 520, 2630–2646.
39. Yu, H.P., and Chaudry, I.H. (2009). The role of estrogen and receptor agonists in maintaining organ function after trauma-hemorrhage. *Shock* 31, 227–237.
40. Angele, M.K., Schneider, C.P., and Chaudry, I.H. (2008). Bench-to-bedside review: latest results in hemorrhagic shock. *Crit. Care* 12, 218.
41. Choudhry, M.A., and Chaudry, I.H. (2008). 17beta-Estradiol: a novel hormone for improving immune and cardiovascular responses following trauma-hemorrhage. *J. Leukoc. Biol.* 83, 518–522.
42. Choudhry, M.A., Schwacha, M.G., Hubbard, W.J., Kerby, J.D., Rue, L.W., Bland, K.I., and Chaudry, I.H. (2005). Gender differences in acute response to trauma-hemorrhage. *Shock* 24 Suppl 1, 101–106.
43. Kawasaki, T., and Chaudry, I.H. (2012). The effects of estrogen on various organs: therapeutic approach for sepsis, trauma, and reperfusion injury. Part I: central nervous system, lung, and heart. *J. Anesth.* 26, 883–891.
44. Akabori, H., Moeinpour, F., Bland, K.I., and Chaudry, I.H. (2010). Mechanism of the anti-inflammatory effect Of 17beta-estradiol on brain following trauma-hemorrhage. *Shock* 33, 43–48.

Address correspondence to:

*Irshad H. Chaudry, PhD*

*Center for Surgical Research*

*Department of Surgery*

*University of Alabama at Birmingham*

*1670 University Boulevard*

*Volker Hall, Room G094*

*Birmingham, AL 35294*

*E-mail: IChaudry@uab.edu*